

## INVESTIGATIONS OF COMPLEX MODES IN A GENERALIZED BILATERAL FINLINE WITH MOUNTING GROOVES AND FINITE CONDUCTOR THICKNESS

Weyl-Kuo Wang, Ching-Kuang C. Tzuang,  
Chun-Yi Shih, and Te-Hui Wang

Institute of Communication Engineering  
National Chiao Tung University, Hsinchu, Taiwan, R.O.C.

## ABSTRACT

A generalized bilateral finline with mounting grooves and finite conductor thickness is analyzed by full-wave mode-matching method. The final nonstandard eigenvalue equation is derived from unknown coefficients in two slot regions. Both relative and absolute convergence analyses of complex modes are performed. The field patterns along the metallized strips are investigated for relative convergence studies. Once the optimal ratios of the numbers of expansion terms among different regions are decided, the absolute convergence study is initiated to obtain the minimal number of total modal expansion terms to save computer time. The validity of this approach is confirmed by checking the available complex mode data. Finally, the dispersion characteristics of fundamental, higher order, evanescent, and complex modes are presented for an asymmetric bilateral finline.

## INTRODUCTION

Since the introduction of finline in 1972 [1], it has become one important class of transmission lines in MMIC. Practical implementations of finlines often encounter discontinuity problems. Many rigorous analytical techniques have been developed, e.g. the spectral domain analysis [2], the transverse resonance technique [3], and the modal expansion concept (or the generalized scattering matrix) [4-6]. Papers in [2] to [6] dealt with ideal finlines either consisting of infinitely thin metallizations or without mounting grooves. As pointed out in [7], the influence of metallization thickness and mounting grooves can be pronounced at higher millimeter-wave frequencies. The only method reported to solve the generalized finline (Fig.1) with mounting grooves and metallization thickness is the generalized transverse resonance method [8,9]. This method requires an identical number of eigenfunction expansions in each region. It is plausible to speculate that relative convergence problem may occur by using this method. The existence of complex modes has not been reported in such generalized finlines. Reference [4] concluded that severe errors could occur even if only one pair of complex modes are neglected when analyzing the finline step discontinuity problem.

It is therefore important to analyze the generalized finline considering the influence of finite metallization thickness and mounting grooves on the dispersion characteristics of the fundamental, higher order, evanescent, and complex modes for accurate analysis of a practical finline discontinuity problem.

This paper analyzes the generalized finline configuration by the mode-matching method and considers the associated relative convergence problem [10]. The relative convergence study discusses various ratios of numbers of eigenfunction expansions in different regions.

A systematic procedure is presented to obtain the optimal choice of the ratios before proceeding to absolute convergence study for modal field solutions. In particular, both relative and absolute convergence studies are reported for complex modes.

## METHOD OF ANALYSIS : MODE-MATCHING METHOD

The generalized finline shown in Fig.1 with each region arbitrarily extending in both x and y directions is analyzed.

Assuming the factor  $e^{j\omega t - \gamma z}$ , where  $\gamma = \alpha + j\beta$ , the rigorous full-wave hybrid TE-to-z and TM-to-z formulation can be expressed as

Region-1 :

$$\Psi^{(1)} = e^{-\gamma z} \sum_{n=1}^{N_1} A_n f_s^{(1)}(y) \sin(kx_n^{(1)} x) \quad \text{Eq.(1a)}$$

Region=j, j= 2, 3, 4;

$$\begin{aligned}\phi^{(j)} &= e^{-\gamma z} \sum_{n=1}^{N_j} f s_n^{(j)}(y) \left\{ F_{en}^{(j)} \sin[kx_n^{(j)}(x-x_\ell^{(j)})] \right. \\ &\quad \left. + G_{en}^{(j)} \cos[kx_n^{(j)}(x-x_\ell^{(j)})] \right\} \\ \Psi^{(j)} &= e^{-\gamma z} \sum_{n=0}^{N_j} f c_n^{(j)}(y) \left\{ F_{hn}^{(j)} \sin[kx_n^{(j)}(x-x_\ell^{(j)})] \right. \\ &\quad \left. + G_{hn}^{(j)} \cos[kx_n^{(j)}(x-x_\ell^{(j)})] \right\}\end{aligned}\quad \text{Eq.(1b)}$$

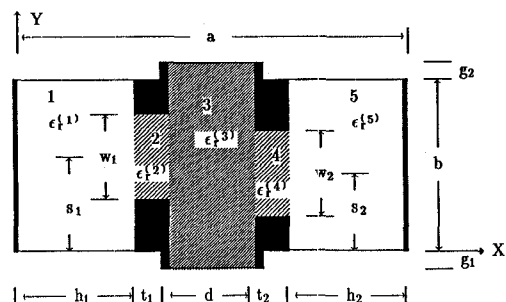


**Fig.1** The generalized finline with grooves and finite metallization thickness.

Region-5 :

$$\begin{aligned}\phi^{(5)} &= e^{-\gamma z} \sum_{n=1}^{N_5} C_n f s_n^{(5)}(y) \sin[kx_n^{(5)}(a-x)] \\ \Psi^{(5)} &= e^{-\gamma z} \sum_{n=0}^{N_5} D_n f c_n^{(5)}(y) \cos[kx_n^{(5)}(a-x)]\end{aligned}\quad \text{Eq.(1c)}$$

where

$$\begin{aligned}f s_n^{(j)}(y) &= \sin\left[n\pi\left(\frac{y-y_{\ell}^{(j)}}{\ell_y^{(j)}}\right)\right] \\ f c_n^{(j)}(y) &= \cos\left[n\pi\left(\frac{y-y_{\ell}^{(j)}}{\ell_y^{(j)}}\right)\right] / \sqrt{1+\delta_{mn}} \\ kx_n^{(j)} &= [\epsilon_r^{(j)} k_0^2 - \left(\frac{n\pi}{\ell_y^{(j)}}\right)^2 + \gamma^2]^{\frac{1}{2}} \\ k_0^2 &= \omega^2 \mu_0 \epsilon_0 \quad \delta_{mn} = \begin{cases} 1 & m=n \\ 0 & m \neq n \end{cases}\end{aligned}$$

and  $N_j$  is the number of eigenfunction expansion terms in region-j.  $(x_{\ell}^{(j)}, y_{\ell}^{(j)})$  and  $\ell_y^{(j)}$  represent the coordinates of the lower-left corner and the length in y-direction of region-j, respectively.

Eq.(1a) to Eq.(1c) indicate that sixteen sets of coefficients exist. There are sixteen interface conditions to be satisfied at  $x=h_1$ ,  $(h_1+t_1)$ ,  $(h_1+t_1+d)$ , and  $(h_1+t_1+d+t_2)$ . Field coefficients in regions other than the slots can be expressed in terms of the eight sets of coefficients in the slots. In this way, the final matrix size is minimized. When all the interface boundary conditions are satisfied, the nonstandard eigenvalue equation looks like

$$\left[ \begin{array}{|c|c|c|c|} \hline [V_{11}] & [V_{12}] & [V_{13}] & [V_{14}] \\ \hline \hline [V_{21}] & [V_{22}] & [V_{23}] & [V_{24}] \\ \hline \hline [V_{31}] & [V_{32}] & [V_{33}] & [V_{34}] \\ \hline \hline [V_{41}] & [V_{42}] & [V_{43}] & [V_{44}] \\ \hline \end{array} \right] \left[ \begin{array}{|c|c|c|c|} \hline F_e^{(2)} \\ \hline G_e^{(2)} \\ \hline F_h^{(2)} \\ \hline G_h^{(2)} \\ \hline F_e^{(4)} \\ \hline G_e^{(4)} \\ \hline F_h^{(4)} \\ \hline G_h^{(4)} \\ \hline \end{array} \right] = 0 \quad \text{Eq.(2)}$$

## RESULTS

### Relative Convergence Study

Fig.2 plots the aperture field  $E_y$  evaluated at  $x=h_1+t_1$  and  $0 \leq y \leq b$ . Fig.2-(a) to Fig.2-(d) correspond to different test conditions. Since the ratio of  $w_1$  to  $w_2$  is nearly three, the ratio of  $N_2$  to  $N_4$  is kept three and their numbers fixed, i.e.  $N_2=30$  and  $N_4=10$ . This assumption is based on the experience gained by [6] and will be justified later. It is clear that Fig.2-(a) and Fig.2-(b) have fairly poor field matchings. When Fig.2-(c) and Fig.2-(d) are overlaid, the aperture fields evaluated at  $x=(h_1+t_1)^+$  make no distinction. The only difference is the fields evaluated at  $x=(h_1+t_1)^-$ . The aperture field  $E_y$  near the corners of the metallic strips, i.e.  $y=s_1 \pm \frac{w_1}{2}$ , should have

$\rho^{-0.476}$  singularity [12],  $\rho$  is the distance from each corner. Fig.2-(d) has smaller slopes at the edges than Fig.2-(c). It is hard to define the slopes since the modal field solutions converge in the mean by the modal expansion technique. However, Fig.2-(c) represents the best choice under the test conditions in terms of field matching and slopes at edge singularities. Notice that the ratio of  $N_1$  to  $N_2$  is nearly the same as that of  $b$  to  $w_1$ .

To justify the assumption of  $N_2$  to  $N_4$  ratio in Fig.2, Fig.3 plots the aperture field  $E_y$  at the slot in region-2. Keeping the ratio of  $N_1$  to  $N_2$  constant while varying  $N_4$ , the results indicate that aperture field  $E_y$  is nearly the same away from the edges (Fig.3-(a)) and differs significantly when approaching the edges (Fig.3-(b)). As  $N_4$  increases from 2 to 10, the aperture field plots start to converge into one line, this justifies the assumption that the ratio of  $N_2$  to  $N_4$  be equal to that of  $w_1$  to  $w_2$ .

Since the propagation constant is the most important parameter for the present study, Fig.4-(a) and (b) show the results which investigates the relative convergence of the normalized propagation constant of one of the complex modes. Both plots indicate that  $\alpha/k_0$  and  $\beta/k_0$  converge sharply at  $N_4=2$  and slowly near  $N_4=10$ .

It is justifiable to conclude that the ratios of the numbers of modal expansion terms between various regions should be approximately the same as those of the corresponding aspect ratios at various regions.

### Absolute Convergence Study

The relative convergence study requires that  $N_2/N_4 \leq 3$  and  $N_1/N_4 \leq 4.6$ . Fig.5-(a) and (b) are the results of the absolute convergence study for one of the complex modes using  $N_1$  as abscissa. For both the real and the imaginary parts of the complex propagation constant, the solid dotted symbols which abide the rule for relative convergence, converge quickly as  $N_1$  increases. Abiding the rule for relative convergence, the solution for the complex modes is still fairly close to the converged solution when only a few number of terms are used.

### Dispersion characteristics of fundamental, higher order, evanescent, and complex modes in a generalized bilateral finline with mounting grooves and finite metallization thickness.

The validity of the above convergence studies and formulations of the mode-matching method is checked against the existing data [11] for complex modes in a symmetric unilateral finline which is the limiting case of the generalized finline. Fig.6 shows that little discrepancies occur around 29 GHz and 10 GHz. Since all the structural parameters are the same except that a metallization thickness of one mil is assumed here, the discrepancies are perhaps due to the effect of finite conductor thickness.

Finally, the normalized propagation constant versus frequency for an asymmetric bilateral finline with mounting grooves and finite metallization thickness is presented in Fig.7. Notice that the relative dielectric constant is ten, much lower than what reference [11] had used. A few regions of complex modes exist in full W-band (75–110 GHz). The third and fourth higher order modes have split into complex modes already.

## CONCLUSION

The existence of complex modes in generalized bilateral finline with mounting grooves and finite

metallization thickness has been reported. In the particular bilateral finline analyzed, the higher order modes just below cutoff may degenerate into complex modes. The propagating-to-evanescent-to-complex or evanescent-to-complex-to-evanescent mode conversions occur throughout full W-band.

The presented convergence studies provide a guideline to determine the numbers of modal expansion terms used in the millimeter-wave CAD program.

## REFERENCES

- [1] P.J.Meier, IEEE MTT-S Digest, 1972, pp. 221-223.
- [2] Q.Zhang and T.Itoh, IEEE Trans., Vol. MTT-35, pp. 138-150, Feb. 1987.
- [3] R. Sorrentino and T. Itoh, IEEE Trans., Vol. MTT-32, pp. 1633-1638, Dec. 1984.
- [4] A. S. Omar and K. Schünemann, IEEE Trans., Vol. MTT-34, pp. 1508-1514, Dec. 1986.
- [5] H. Helard, J. Citerne, Q. Picon, and V. F. Hanna, IEEE MTT-S Digest, 1983, pp. 387-389.
- [6] R. R. Mansour and R. H. Macphie, IEEE Trans., Vol. MTT-34, pp. 1490-1498, Dec. 1986.
- [7] R. Vahldieck and W. J. R. Hoefer, IEEE MTT-S Digest, 1985, pp. 143-144.
- [8] R. Vahldieck, IEEE Trans., Vol. MTT-32, pp. 1454-1460, Nov. 1984.
- [9] J. Bornemann and F. Arndt, IEEE Trans., Vol. MTT-34, pp. 85-92, Jan. 1986.
- [10] T. S. Chu and T. Itoh, IEEE Trans., Vol. MTT-33, pp. 1018-1023, Oct. 1985.
- [11] A. S. Omar and K. Schünemann, IEEE Trans., Vol. MTT-33, pp. 1313-1322, Dec. 1985.
- [12] Meixner, J., IEEE Trans., Vol. AP-20, pp. 442-446, 1972.

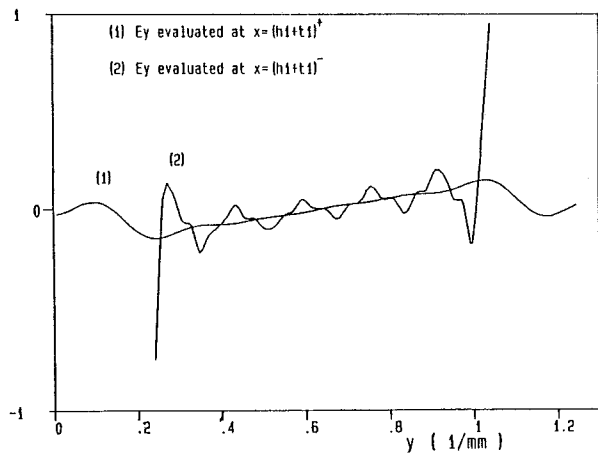


Fig.2 (a)

**Fig.2** Relative convergence studies of the aperture field  $E_y$  evaluated at  $x=h_1+t_1$  and  $0 \leq y \leq b$ . Structural parameters :  $f=70$  GHz,  $\epsilon_r^{(3)}=12$ ,  $\epsilon_r^{(1)}=\epsilon_r^{(2)}=\epsilon_r^{(4)}=\epsilon_r^{(5)}=1$ ,  $a=2.032$  mm,  $b=1.27$  mm,  $d=32\%b$ ,  $t_1=t_2=1$  mil,  $w_1=64\%b$ ,  $w_2=22\%b$ ,  $s_1=s_2=b/2$ ,  $d_m=0.85$  mm,  $g_1=g_2=0$   
 (a)  $N_1=N_3=N_5=16$   $N_2=30$   $N_4=10$   
 (b)  $N_1=N_3=N_5=30$   $N_2=30$   $N_4=10$   
 (c)  $N_1=N_3=N_5=46$   $N_2=30$   $N_4=10$   
 (d)  $N_1=N_3=N_5=60$   $N_2=30$   $N_4=10$

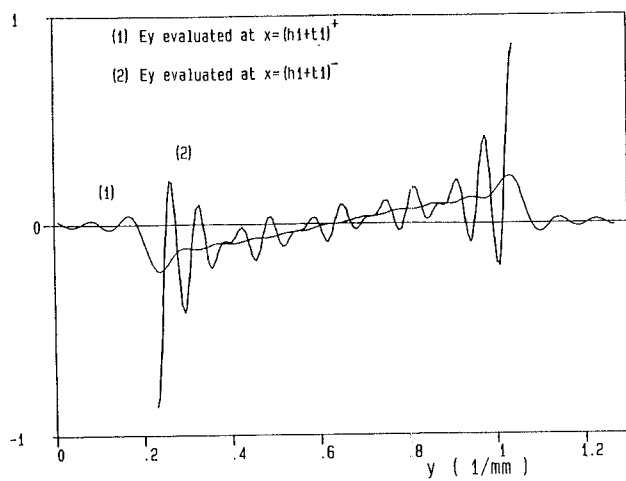


Fig.2 (b)

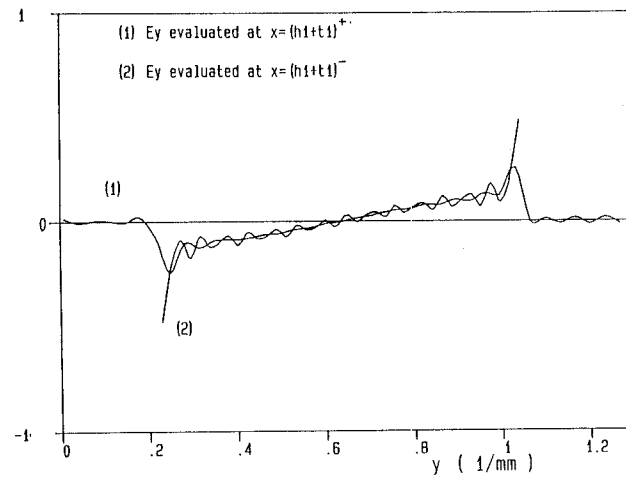


Fig.2 (c)

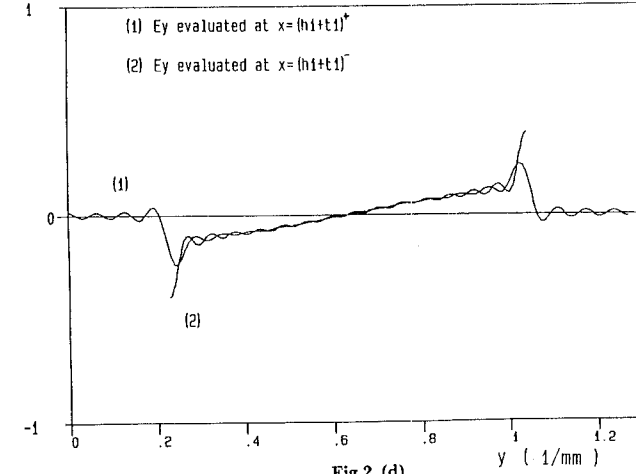
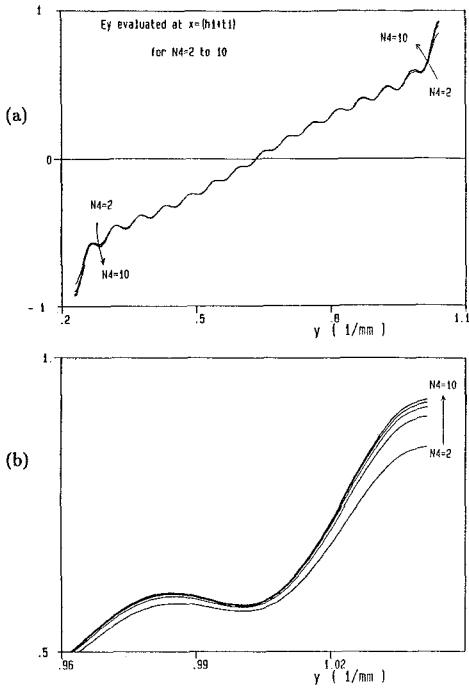
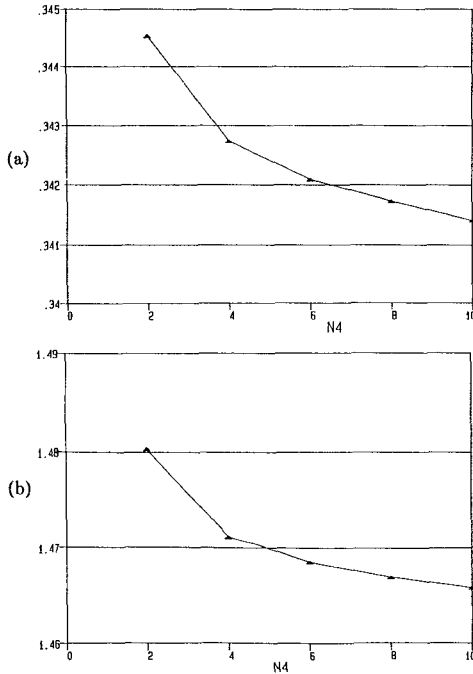


Fig.2 (d)



**Fig.3** Relative convergence studies of aperture field  $E_y$  evaluated at  $x=h_1+t_1$  and  $(s_1-\frac{w_1}{2}) \leq y \leq (s_1+\frac{w_1}{2})$ . Structural parameters : same as Fig.2  
 (a)  $N_1=N_3=N_5=46$   $N_2=30$   $N_4=2,4,6,8,10$   
 (b) Expanded view (a) near  $y=s_1+\frac{w_1}{2}$



**Fig.4** Relative convergence studies of a normalized propagation constant of complex modes. Test condition : same as in Fig.3  
 (a)  $\beta/k_0$  versus  $N_4$  (b)  $\alpha/k_0$  versus  $N_4$

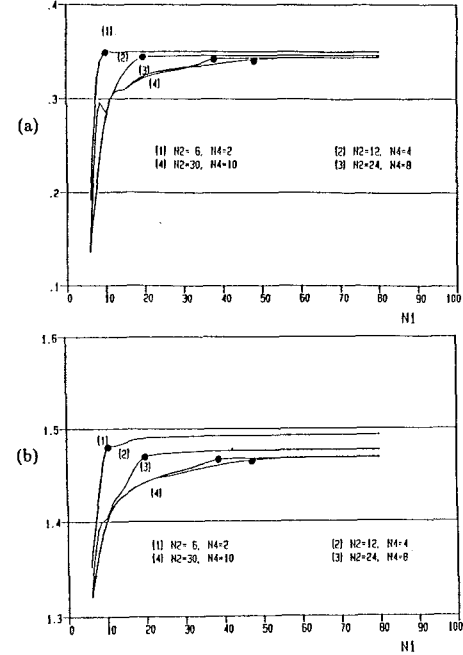


**Fig.5** Absolute convergence studies of the normalized propagation constant of one of the complex modes  
 (a)  $\beta/k_0$  versus  $N_1$  (b)  $\alpha/k_0$  versus  $N_1$

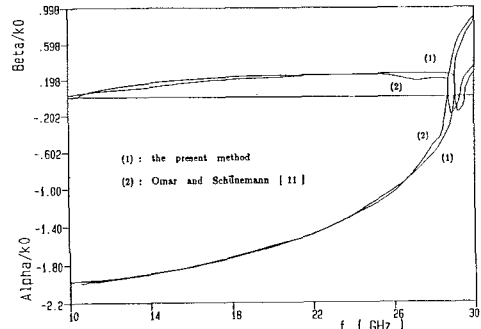


**Fig.6** Validity check of the normalized propagation constant of complex modes of a symmetric unilateral finline versus frequency.

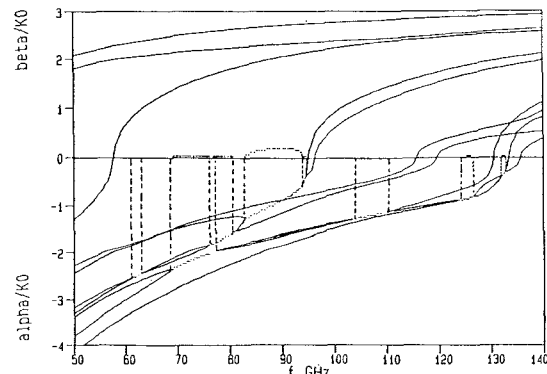


**Fig.7** Normalized propagation constant versus frequency for an asymmetric bilateral finline.  $a=2.54\text{mm}$ ,  $b=1.27\text{mm}$ ,  $\epsilon_r^{(3)}=10$ ,  $\epsilon_r^{(1)}=\epsilon_r^{(2)}=\epsilon_r^{(4)}=\epsilon_r^{(5)}=1$ ,  $d=30\%b$ ,  $t_1=t_2=0.7\text{ mil}$ ,  $w_1=30\%b$ ,  $w_2=45\%b$ ,  $s_1=65\%b$ ,  $s_2=57.5\%b$ ,  $d_m=42.5\%a$ ,  $g_1=g_2=2.5\text{ mils}$ .